ISSN 1063-7834, Physics of the Solid State, 2015, Vol. 57, No. 2, pp. 266–269. © Pleiades Publishing, Ltd., 2015.
Original Russian Text © E.A. Golovkova, A.V. Surkov, G.F. Syrykh, 2015, published in Fizika Tverdogo Tela, 2015, Vol. 57, No. 2, pp. 254–257.

METALS

Crystallization of Amorphous Zr–Be Alloys

E. A. Golovkova, A. V. Surkov, and G. F. Syrykh

National Research Centre "Kurchatov Institute," pl. Akademika Kurchatova 1, Moscow, 123098 Russia
e-mail: amorphous2014@gmail.com

Received August 13, 2014

Abstract—The thermal stability and structure of binary amorphous $Zr_{100-x}Be_x$ alloys have been studied using differential scanning calorimetry and neutron diffraction over a wide concentration range ($30 \le x \le 65$). The amorphous alloys have been prepared by rapid quenching from melt. The studied amorphous system involves the composition range around the eutectic composition with boundary phases α-Zr and $ZrBe_2$. It has been found that the crystallization of alloys with low beryllium contents ("hypoeutectic" alloys with $x \le 40$) proceeds in two stages. Neutron diffraction has demonstrated that, at the first stage, α-Zr crystallizes and the remaining amorphous phase is enriched to the eutectic composition; at the second stage, the alloy crystallizes in the α-Zr and $ZrBe_2$ phases. At higher beryllium contents ("hypereutectic" alloys), one phase transition of the amorphous phase to a mixture of the α-Zr and $ZrBe_2$ phases has been observed. The concentration dependences of the crystallization temperature and activation energy have been revealed.

DOI: 10.1134/S1063783415020122

1. INTRODUCTION

The physical and technological properties of amorphous metallic Zr–Be alloys attract attention of researchers as before. These properties are of interest from the fundamental and applied standpoints. Metallic Zr–Be glasses consist of components incommensurable with each other in atomic radii and masses and can be obtained over a wide concentration range, which facilitates the study of their atomic structures and dynamics, in particular, acoustic and optical modes [1–4].

The Zr–Be amorphous alloy ribbons several tens of micrometers in thickness can be used as a solder in diffusion welding of Zr parts for atomic industry. This can be alternative to the method of beryllium sputtering on the surface of a zirconium part, which is costly and harmful to the environment [5].

In [6], the thermal stability of amorphous $Zr_{100-x}Be_x$ alloys was studied using differential scanning calorimetry (DSC) and X-ray diffraction in a limited concentration range $30 < x < 50$. The DSC data revealed two exothermal peaks for the samples with $x \le 40$. The X-ray diffraction study showed that the α-Zr phase is formed at the first crystallization stage. It was assumed in [6] that the remaining amorphous phase is enriched in zirconium to the composition $ZrBe_2$, which crystallizes at the second stage. In samples with $x > 40$, phases α-Zr and $ZrBe_2$ crystallize simultaneously. The dependence of the crystallization temperatures and activation energies on the beryllium concentration was not observed.

Differential scanning calorimetry and X-ray diffraction were also used to study the thermal stability of a number of amorphous metal–metalloid alloys near their eutectic compositions [7, 8]. "Hypoeutectic" amorphous alloys crystallize in two stages. It was also concluded that, first, the pure metal crystallizes, and the remaining amorphous phase is enriched to the composition of a metastable crystalline compound (Ni–B system) [7] or to the composition of a stable crystalline compound, i.e., the second boundary phase (Co–B,Si system) [8].

To better understand the processes of crystallization of metallic glasses, we performed the DSC and neutron diffraction investigations of the $Zr_{100-x}Be_x$ system over a wider concentration range ($30 \le x \le 65$). Unlike X-rays, the amplitudes of neutron scattering by Zr and Be are almost equal to each other, which facilitates the phase analysis of the sample after the first crystallization stage.

2. SAMPLE PREPARATION AND EXPERIMENTAL TECHNIQUE

Samples of the amorphous $Zr_{100-x}Be_x$ alloys with $x = 30$, 40, 50, 55, 60, and 65 were prepared by rapid quenching from melt on a rotating copper disc in a purified argon atmosphere. The amorphous state was confirmed by neutron diffraction on a DISK diffractometer installed on an IR-8 reactor at the National Research Centre "Kurchatov Institute" (Moscow, Russia). The obtained structure factors $S(Q)$ are shown in Fig. 1. It is seen that the peaks systematically shift toward increase in the momentum transfer as the beryllium concentration increases. The reason is that partial structure factors $S(Q)_{Zr-Zr}$, $S(Q)_{Zr-Be}$, and $S(Q)_{Be-Be}$ are markedly different because of the large

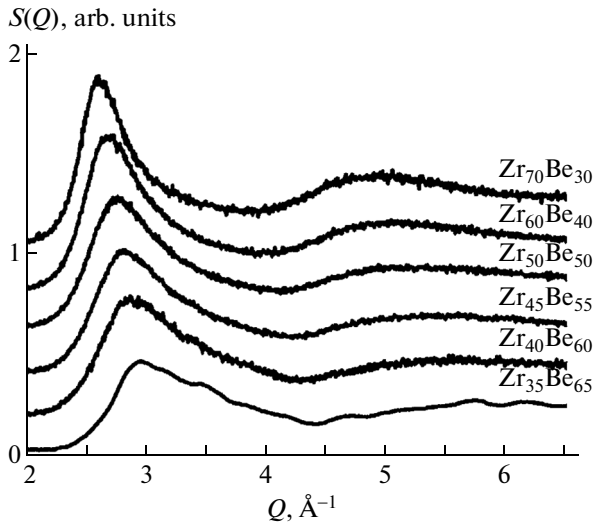

Fig. 1. Structure factors $S(Q)$ of the amorphous $Zr_{100-x}Be_x$ system with $x = 30$, 40, 50, 55, 60, and 65. For convenience, the curves are shifted along the ordinate axis.

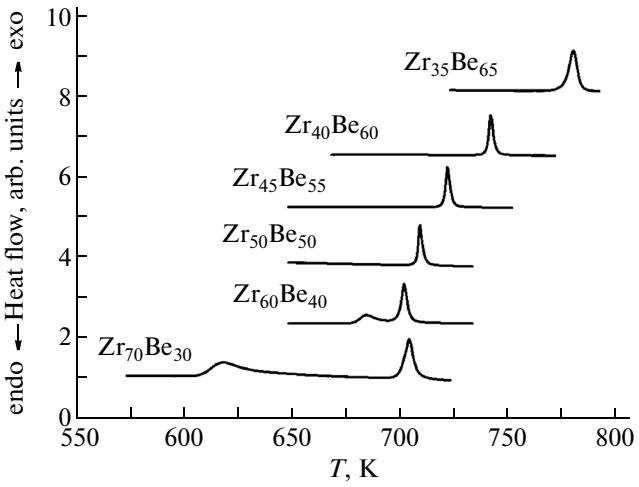

Fig. 2. DSC data for the amorphous $Zr_{100-x}Be_x$ system with $x = 30$, 40, 50, 55, 60, and 65. For convenience, the curves are shifted along the ordinate axis.

difference in the zirconium and beryllium ionic radii [1, 2]. Thus, the neutron diffraction data are very sensitive to the sample composition. It should be noted that the X-ray diffraction data for these samples are slightly dependent on the concentration, because X-rays are predominantly scattered by zirconium.

The crystallization of the samples was studied using DSC on a NETZSCH STA 449 C thermal analyzer. The measurements were carried out at four heating rates: 10, 20, 30, and 40 K/min. Figure 2 shows the DSC curves measured at a heating rate of 20 K/min. The DSC curves of the $Zr_{100-x}Be_x$ samples with $x = 30$ and 40 have two exothermal peaks, whereas the DSC curves of the $Zr_{100-x}Be_x$ samples with $x = 50$, 55, 60, and 65 have one exothermal peak. The positions of these peaks systematically shift with variations in the beryllium concentration. We measured the structure factor for the $Zr_{70}Be_{30}$ sample that was rapidly cooled after the first crystallization stage (Fig. 3). The peaks are observed corresponding to the crystalline state of zirconium and zirconium-rich amorphous phase. To estimate the amorphous phase composition, we also show in Fig. 3 the structure factors of samples $Zr_{60}Be_{40}$ and $Zr_{35}Be_{65}$. The activation energies (ΔE_x) of the reactions of crystallization were determined by the Kissinger method [9]

$$d\ln(n/T_x)/d(1/T_x) = -\Delta E_x/R,$$

where n is the heating rate, T_x is the temperature of the peak in the DSC curve, and R is the universal gas constant. The Kissinger plots for the first and second reactions of crystallization are shown in Fig. 4.

Figure 5a shows the dependence of the crystallization temperature on beryllium content x in the alloy (the dashed lines show a part of the Zr–Be phase diagram [10]). Figure 5b shows the activation energies as functions of beryllium content x in the alloy.

3. DISCUSSION OF THE RESULTS

According to [11], depending on the concentration, the amorphous phase can crystallize according to one of the following scenarios: the preferred crystallization of one of the phases and the enrichment of the remaining amorphous phase, the polymorphic (without any change in the concentration) crystallization,

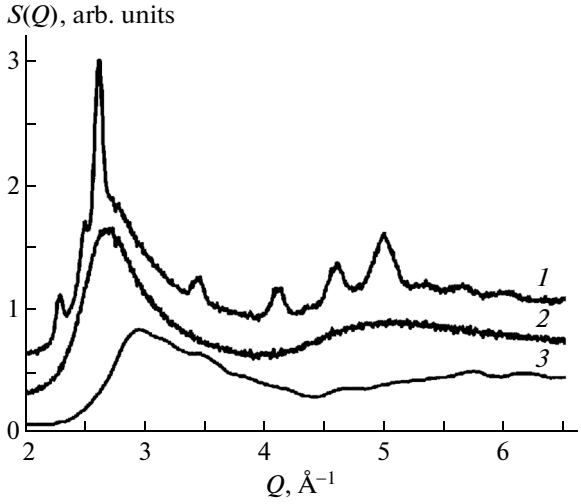

Fig. 3. Structure factors $S(Q)$: (*1*) $Zr_{70}Be_{30}$ sample after the first crystallization stage, (2) initial amorphous $Zr_{60}Be_{40}$ sample, and (*3*) initial amorphous $Zr_{35}Be_{65}$ sample. For convenience, the curves are shifted along the ordinate axis.

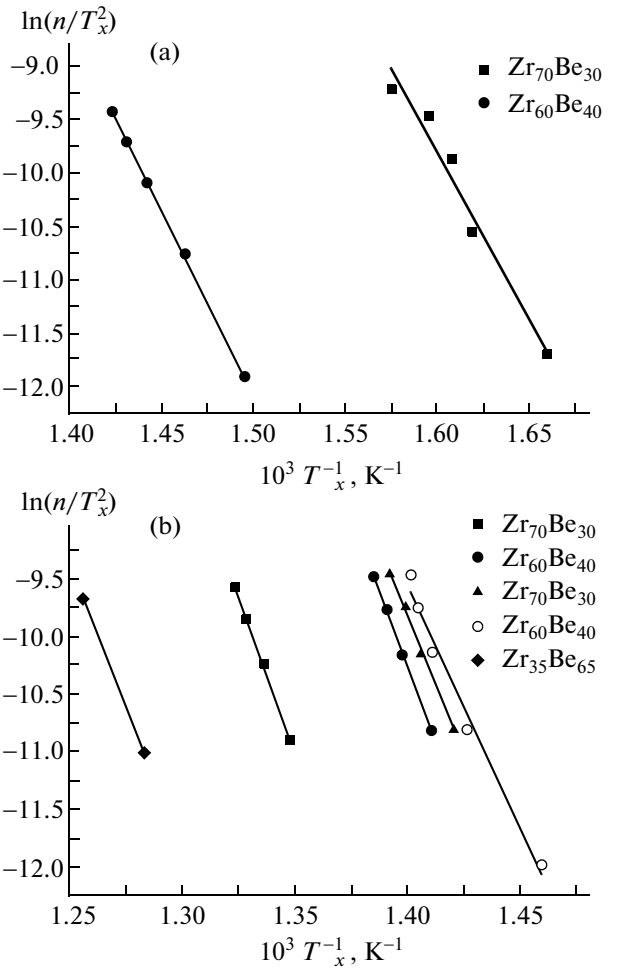

Fig. 4. Kissinger plots for the amorphous $Zr_{100-x}Be_x$ system with $x = 30$, 40, 50, 60, and 65: (a) the first stage of crystallization and (b) the second stage of crystallization.

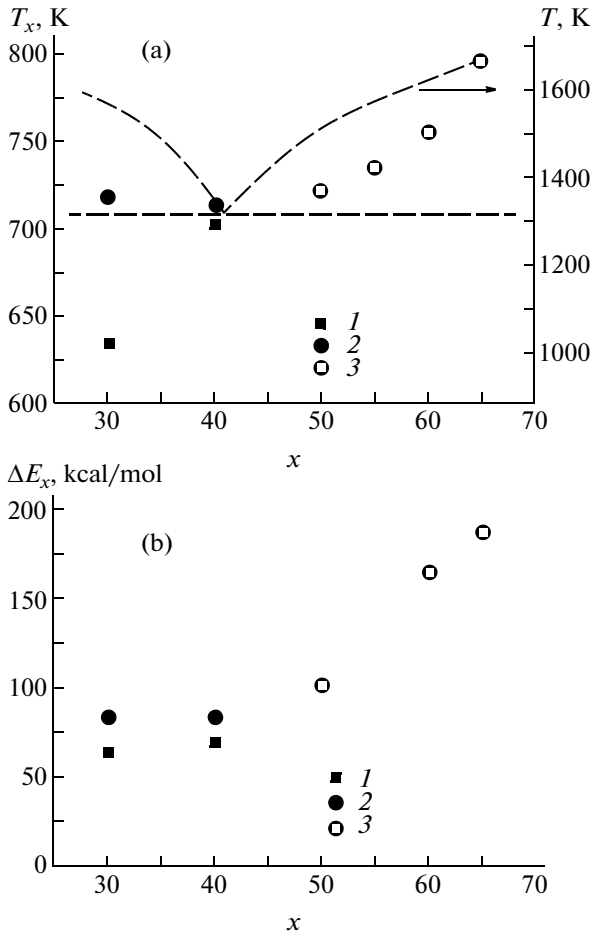

Fig. 5. (a) Concentration dependence of the crystallization temperature of the (*1*) first and (*2*) second stages for the "hypoeutectic" composition and (*3*) "hypereutectic" composition. The dashed lines show the conventional Zr–Be phase diagram. (b) Concentration dependence of the crystallization activation energy of the (*1*) first and (*2*) second stages for the "hypoeutectic" composition and (*3*) "hypereutectic" composition. x is the Be concentration.

and the eutectic (simultaneous) crystallization of both phases.

As follows from Fig. 3, at the first stage, the α-Zr phase preferentially crystallizes, and the enriched amorphous phase composition is closer to the eutectic composition ($Zr_{60}Be_{40}$) than to the composition of the second boundary phase $ZrBe_2$, as was argued in [6]. The enriched amorphous phase crystallites in phases α-Zr and $ZrBe_2$ according to the eutectic type at the second stage of crystallization.

An analysis of the concentration dependence of the crystallization activation energy (Fig. 5b) shows that the crystallization activation energy of phase α-Zr in "hypoeutectic" alloys is lower (the first stage) than that of amorphous phase of the eutectic composition (the second stage): 63.1 and 83.5 kcal/mol, respectively. In this case, the crystallization temperature and activation energy of phase α-Zr increase as the eutectic composition is approached, which can be explained by the decrease in the number of frozen-in α-Zr crystallization centers. The amorphous $Zr_{35}Be_{65}$ sample is close in composition to the crystalline $ZrBe_2$ phase. Therefore, the crystallization of this sample is polymorphic with higher crystallization activation energy and crystallization temperature (187.1 kcal/mol and 796 K, respectively) than those for the eutectic composition (83.5 kcal/mol and 714 K). These parameters have intermediate values for $Zr_{50}Be_{50}$ and $Zr_{40}Be_{60}$ alloy, and this fact can be explained by the quantitative proportion of the eutectic and phase $ZrBe_2$ in them. We call attention on the "mirror correlation" between the crystallization temperature of the amorphous phase and that of the liquid phase of the "hypoeutectic" alloys (Fig. 5a). In both cases, first, the pure metal crystallizes, and the amorphous and liquid phases are enriched to the eutectic composition that crystallizes during the second stage.

4. CONCLUSIONS

Thus, the neutron diffraction data show that, at the first stage of crystallization of "hypoeutectic" amorphous Zr–Be alloys, The preferred crystallization occurs with precipitation of the α-Zr phase and enrichment of the remaining amorphous phase to the eutectic composition. During the second stage, the enriched amorphous phase crystallizes in phases α-Zr and $ZrBe_2$.

The "hypereutectic" alloys do not demonstrate preferred crystallization of the second boundary $ZrBe_2$ phase, because it can exist in the amorphous state with high activation energy of crystallization. Therefore, these alloys simultaneously crystallize in a mixture of the boundary α-Zr and $ZrBe_2$ phases.

It can be assumed that similar crystallization is also characteristic of metal–metalloid systems.

ACKNOWLEDGMENTS

This study was supported by the Russian Foundation for Basic Research (project no. 12-02-00705-a).

REFERENCES

1. A. M. Bratkovskii, S. L. Isakov, S. N. Ishmaev, I. P. Sadikov, A. V. Smirnov, G. F. Syrykh, M. N. Khlopkin, and N. A. Chernoplekov, Sov. Phys. JETP **73** (4), 772 (1991).
2. M. Maret, C. N. J. Wagner, G. Etherington, A. Soper, and L. E. Tanner, J. Phys. (Paris) **47**, 863 (1986).
3. G. F. Syrykh, A. S. Ivanov, N. A. Klimenko, Yu. V. Lisichkin, H. Mutka, and J. A. Stride, J. Phys.: Condens. Matter **20**, 104241 (2008).
4. G. F. Syrykh, N. V. Situkha, N. A. Klimenko, and J. A. Stride, J. Surf. Invest. **5** (3), 409 (2011).
5. J. Amato, F. Baudrocco, and M. Ravizza, Welding J. **51**, 341 (1972).
6. C. H. Park, Y. S. Han, Y. K. Kim, K. J. Jang, J. Y. Lee, C. B. Choi, and K. S. Sim, J. Nucl. Mater. **254**, 34 (1998).
7. M. Vatsuura, Solid State Commun. **30**, 231 (1979).
8. E. Jakubszyk, Z. Mandecki, and M. Jakubczyk, J. Non-Cryst. Solids **232–234**, 453 (1998).
9. H. E. Kissinger, Anal. Chem. **29**, 1702 (1957).
10. M. Hansen and K. Anderko, *Constitution of Binary Alloys* (McGraw-Hill, New York, 1958; Metallurgizdat, Moscow, 1962), p. 324.
11. U. Koster and P. Weiss, J. Non-Cryst. Solids **17**, 359 (1975).

Translated by Yu. Ryzhkov